Impact of experimental conditions on material response during forming of steel in semi-solid state

Eric Becker[a], Véronique Favier[b], Regis Bigot[a,*], Pierre Cezard[c], Laurent Langlois[a]

[a] Arts et Métiers ParisTech, CER de Metz, Laboratoire de Conception Fabrication Commande (LCFC), EA 4495, 4 rue Augustin Fresnel, Metz Technopole, 57078 – Metz, France
[b] Arts et Métiers ParisTech, CER de Paris, CNRS UMR 8006, PIMM, 151 bd de l'Hôpital – 75013 Paris, France
[c] Ascometal CREAS, avenue France, F-57300 Hagondange, France

A B S T R A C T

Semi-solid forming is an effective near-net-shape forming process to produce components with complex geometry and in fewer forming steps. It benefits from the complex thixotropic behaviour of semi-solids. However, the consequences of such behaviour on the flow during thixoforming, is still neither completely characterized and nor fully understood, especially for high melting point alloys. The study described in this paper investigates thixoextrusion for C38 low carbon steel material using dies at temperatures much lower than the slug temperature. Four different process parameters were studied: the initial slug temperature, the die temperature, the ram speed and the presence of a ceramic layer at the tool/material interface. The extruded parts were found to have an exact shape and a good surface state only if the temperature was below a certain value. This critical temperature is not an intrinsic material property since its value depends on die temperature and the presence of the Ceraspray©layer. Two kinds of flow were highlighted: a homogeneous flow controlled by the behaviour of the solid skeleton characterized by a positive strain rate sensitivity, and a non homogeneous flow (macro liquid/solid phase separation) dominated by the flow of the free liquid. With decreasing ram speed, heat losses increase so that the overall consistency of the material improves, leading to apparent negative strain rate sensitivity. Finally, some ways to optimise thixoforming are proposed.

1. Introduction

Semi-solid forming is an effective near-net-shape forming process which is particularly well-adapted to producing components with complex geometry and has the advantage of requiring fewer forming steps. Besides, the load required to deform material is much lower than in the case of conventional hot forging due to smaller resistance and good fluidity of the material (Hirt et al., 2009). The behaviour of semi-solids depends not only on the liquid volume fraction but also on the microstructure. As shown by Flemings (1991a,b), it is now well known that a globular microstructure for the solid phase gives a lower viscosity and a more homogeneous flow than a dendritic structure. The solid phase may be connected to form a continuous solid skeleton. In this case, part of the liquid is entrapped within the solid phase and acts as an additional effective solid fraction. When the solid phase is not fully connected, the solid continuous skeleton does not exist anymore. So, the material behaves as a suspension having solid agglomerates. During deformation, many effects such as agglomeration, disagglomeration, and coarsening phenomena of the solid phase change the semi-solid microstructure. As shown by Quaak (1996), Koke and Modigell (2003), when a semi-solid is sheared with a high enough shear rate, solid bonds between solid particles break and may release some entrapped liquid. Bigot et al. (2005) showed again these properties and studied the thermal impact of the process by indentation test. The consequences of such behaviour on the flow during thixoforming in "industrial" context, is still neither completely characterized and nor fully understood, especially for high melting point alloys despite the clear interest of such a forming process. The high fluidity of semi-solid steels enables to produce near-net-shape steel components with complicated geometry in a single-step permanent mould (Hirt et al., 2009). Kapranos et al. (1993) produced thixoforged cog wheels made of M2-tool with a "tooth-to-tooth" distance of 114 mm. Rouff et al. (2002) produced a thixoforged plate made of C38 steel grade, displaying strong variations of the component thickness. Connecting rods and hinge bearings made of steel grade C70S6 were also successfully thixoforged (Puttgen et al., 2007). They showed a good reproduction in shape and surface quality. However, defects such as macroscopic and microscopic incomplete form-filling have been found. They are attributed to premature freezing of the material and non-laminar filling or solidification shrinkage. As mentioned

* Corresponding author. Tel.: +33 3 87 37 54 30; fax: +33 3 87 37 54 70.
E-mail address: regis.bigot@metz.ensam.fr (R. Bigot).

Table 1
C38 chemical composition (wt 10^{-3}%).

C	Mn	P	S	Si	Al	N	Ni	Cr	Cu
418	751	10	21	198	21	65	77	144	133

by Cezard and Sourmail (2008), understanding the impact of strain rate gradient related to the component geometry and of thermal exchanges occurring during the forming process on the flow behaviour remains a big issue. Becker et al. (2009) showed in a recent work the impact of slug temperature on final microstructure for thixoforged parts in steel alloy.

Puttgen et al. (2007) wrote a state-of-the-art on steel thixoforging processes with a focus on technologies in relation to material choice. So liquid/solid diagrams for several steel grades are presented. Cezard and Sourmail (2008) made a synthesis on industrial applications for high melting point alloys. Their work illustrates the challenges encountered in the industrialisation of thixoforging processes. Hirt et al. (2009) summed up works in experimental and numerical fields. The modeling field has been summarized by Atkinson (2005) and Favier et al. (2009).

The present study investigates thixoextrusion for C38 low carbon steel material using dies at temperatures much lower than the slug temperature, which means that the forming process is considered as nonisothermal. Four different process parameters were studied: the initial slug temperature, the die temperature, the ram speed and the presence of a ceramic layer at the tool/material interface. The load–displacement curves as well as the shape of the extruded parts are discussed in relation to the impact of temperature and flow on the microstructure and vice-versa. Finally, some ways to optimise thixoforming are proposed.

2. Experimental procedure

2.1. Slug material

The subject of this work is the investigation of thixoforging for C38 low carbon steel material. The typical chemical composition (per unit mass) of this steel grade is given in Table 1. Rolling bars were cut in slugs of 30 mm in diameter and 45 mm long.

Fig. 1 shows the microstructure of the initial material. The steel alloy contains fine microstructure of ferrite and perlite. The semi-solid state is obtained by partial remelting. The literature works (Omar et al., 2005) showed that prior deformed steel alloys displayed a suitable microstructure for thixoforming when partially remelted even it may be not the conventional globular one. In general, thin liquid films formed at the grain boundaries.

As Balitchev et al. (2004) or Gibbs and Mendez (2008), the liquid fraction/temperature relationship was determined using differential scanning calorimetry (DSC) (Fig. 2). The 15 mg-specimens of about 3 mm in diameter were heated to 1510 °C at 20 °C/min. Fig. 2 shows that the material exhibits a slow increase in liquid fraction for temperatures ranging from 1410 °C to 1450 °C. This temperature range was chosen for thixoforming experiments described in the following. Note that the heating conditions (specimen size, heating rate) for DSC experiments and for thixoforming tests using an induction system are very different. Consequently, the real liquid fraction during the thixoforming route in the slug may be different from the one measured by DSC for a given temperature. The liquid fraction values given in the following are thus approximate, which is why both temperature and liquid fraction are indicated to give more experimental information.

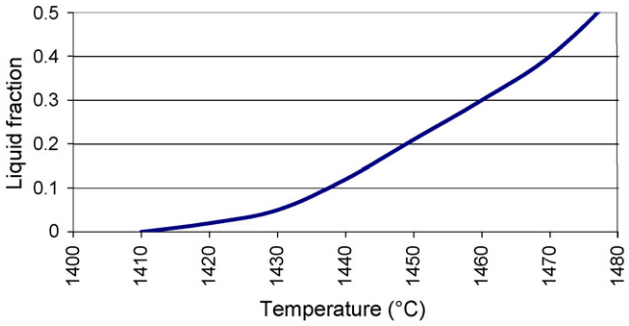

Fig. 2. Liquid fraction versus temperature obtained by DSC (with University of Liège collaboration) (Rouff, 2003).

2.2. Heating device

Jung (2000) and Jung et al. (2000) carried out experiments on inductive system to obtain globular structure for low melting point alloy. In 2003, Kang et al. performed some numerical simulation on inductive system to heat aluminum alloy in semi-solid state. Hirt et al. (2005) used an inductive system to obtain a semi-solid state in a high carbon steel. Rassili et al. (2006) showed a non-cylindrical heating system to obtain a more homogeneous magnetic field and to reduce thermal gradients within the billet. In this work, the slugs were heated in an induction furnace (frequency: 2–30 kHz, power: 25–50 kW). Like Omar et al. (2004, 2005), the heating was done in a protective argon atmosphere to prevent oxidation. Indeed, this oxidation can strongly affect friction phenomena and reduce tool life. The heating route consisted in successive power cycles to ensure a homogeneous temperature in the slug. Typically, the whole heating cycle lasted about 250 s, so that the average heating speed was 350 °C/min. Three thermocouples were inserted in three different places to monitor the temperature uniformity: at the centre of the slug (radial direction) at 22.5 mm in depth; at 7.5 mm from the centre and 12 mm in depth; and at 7.5 mm from the centre and 22.5 mm in depth. The inductor was designed to allow a direct extrusion through the induction box and to avoid a transfer of the slug (Fig. 3).

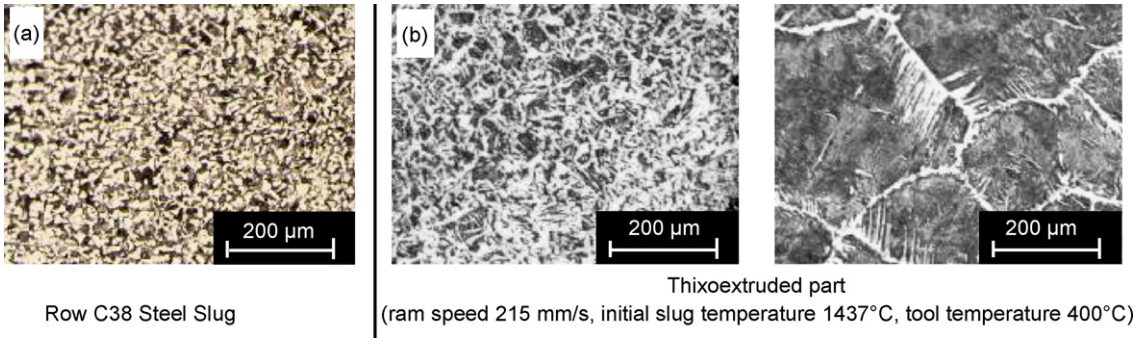

Fig. 1. microstructures of C38 steel: (a) initial slug, (b) at two positions of a thixoforged part.

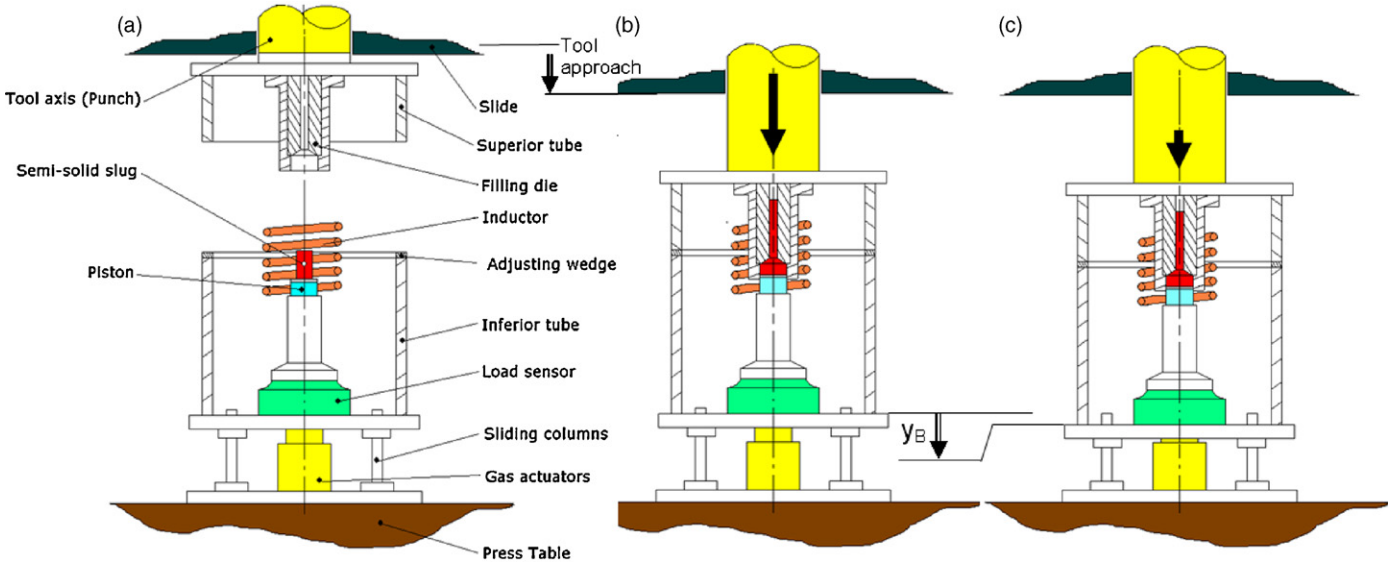

Fig. 3. Complete extrusion device (Arts et Métiers Paristech design) settled on the "ULG" press, (a) heating step before thixoforging, (b) end of thixoforging (the tubes are in contact), and (c) tool deceleration step (dampers compression).

2.3. Extrusion set-up

Fig. 4 shows the principle of the extrusion set-up. The thixoextrusion die was axisymmetric. The container was 40 mm in diameter. The die aperture at the exit is 12 mm in diameter (extrusion ratio = 0.3). The cone angle is 30°. A radial machining at the upper end of the channel is realised to limit pressure during the thixoforming process. The slug was placed on an Inconel©piston. A Nefacier1500©disc (based on ceramic fibres with low content of non-fibrous ceramic particles) was placed between the piston and the slug to reduce heat losses during the induction step. The material of the die was Inconel©and the container was X38CrMoV5 tool steel.

Extrusion tests were carried out using two hydraulic presses in order to change the ram speed range. The first press is located at the "Arts et Métiers ParisTech" Metz and the maximum die filling velocity is 40 mm/s. The second is at the University of Liege and the die filling velocity ranges from 10 mm/s to 750 mm/s. The schematic diagram of the complete thixoforming set-up is shown in Fig. 3. The die (Fig. 3) was designed: (i) to eliminate the heat losses between the heating step and the forming step, (ii) to ensure a constant die filling velocity during thixoextrusion and (iii) to control the filling length. Concerning the first point, it is now well known that the transfer from heating step to forming step leads to temperature losses which generate a lower overall liquid fraction and a non uniform temperature distribution of the slug before thixoforming. The extrusion die was designed to pass through the induction box. Consequently, the transfer step is very strongly reduced. In other words the end of heating corresponds to the start of the forming. Concerning the second point, the upper die stop of the high speed hydraulic press at the University of Liege is not instantaneous because of its "hydraulic" inertia. Hence, the metal is still being deformed while the ram speed decreases. To keep the die filling velocity constant, a damping system was integrated (Becker, 2008). It is composed of four gas actuators, and four sliding columns (Fig. 3). It is placed on the press table and supports the punch. This active part of the tools is also made up of two tubes which transmit the press loading. The upper tube is fixed on the press tool axis and the lower tube is fixed on the damper system. When the two tubes touch, the thixoextrusion is completed. As soon as the two tubes are in contact, the damper table moves to absorb the deceleration stage of the press. Concerning the last point, this device enables to control the filling length by adjusting the length of the lower tube. The whole device is instrumented using load and displacement sensors. The load sensor is placed under the punch and measures the extrusion load exerted on the thixoextruded part. A ceramic particle layer, labelled as Ceraspray©was put on the active parts of the die unless otherwise stated. The effect of the ceramic layer on the thixoforming process is discussed in Section 3.4.

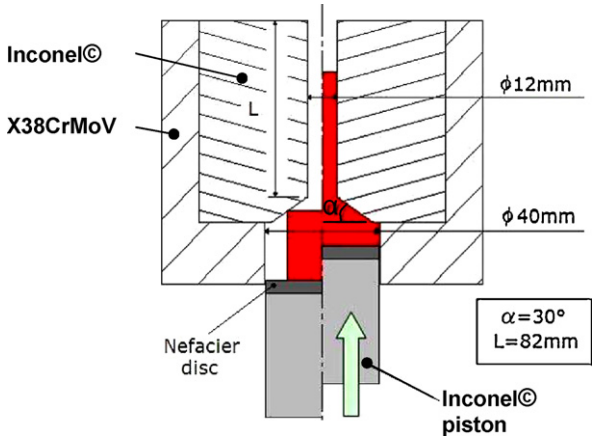

Fig. 4. Principle of the extrusion test.

2.4. Experimental conditions

Experiments were carried out under different conditions (Table 2), as follows:

Table 2
Experimental conditions.

Conditions	Values
Slug temperature	1429–1451 °C
Ram speed	30–215 mm/s
Tool temperature	20–400 °C
Ceraspray©layer	No–Yes

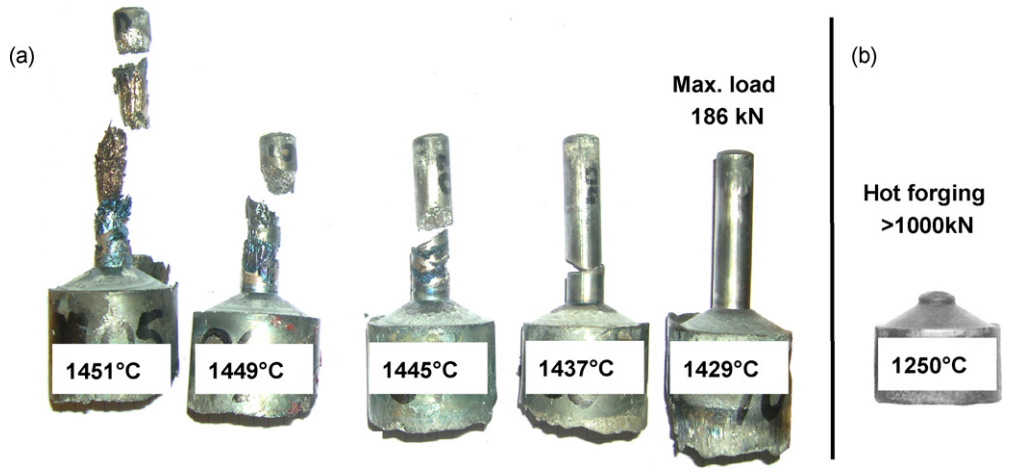

Fig. 5. (a) Parts thixoextruded at various initial slug temperatures with a "cold" die and a ram speed of 215 mm/s. (b) Part hot forged with a slug temperature of 1250 °C, a "cold" die and a ram speed of 30 mm/s.

- *Varying initial temperatures of semi-solids before thixoextrusion*. The initial temperature of the slugs ranged from 1429 °C to 1451 °C. In these experiments, the die filling velocity was held constant and was equal to 215 mm/s and the initial tool temperature was equal to 20 °C.
- *Varying the die filling velocity*: The die filling velocity ranged from 30 mm/s to 215 mm/s. In these experiments, the initial tool temperature was equal to 20 °C. For a set of experiments, the initial slug temperature was held constant and was equal to 1451 °C or 1429 °C.
- *Varying the tool temperature*. Two tool temperatures were used. A thixoforging carried out when the tool temperature is 20 °C is considered as "cold". When the tool temperature reaches 400 °C, it is considered as "warm". The filling die was cooled between each experiment to ensure an identical tool temperature for all the experiments.
- Adding or not a Ceraspray©layer.

3. Results

3.1. Impact of the initial temperature of the slug

Fig. 5 shows five thixoextruded parts forged at 215 mm/s and at initial slug temperatures ranging from 1429 °C to 1451 °C. A bad filling was obtained at 1445 °C, 1449 °C and 1451 °C and the extruded parts displayed wrenching. On the contrary, complete filling was obtained at 1429 °C and 1437 °C. The extruded parts showed the exact shape and a good surface state.

Fig. 6 shows the load–displacement curves associated with the experiments mentioned above. First, the load slowly increases with the displacement: this step is associated with the filling of the container. Then the load increases much more up to a maximum value: this step corresponds to the filling of the die cone, the latter having the smallest diameter up at the end of the extrusion. We observe that the load level clearly increases when the initial slug temperature decreases mainly because of the increase of the solid fraction.

3.2. Impact of the die filling velocity

Fig. 7a shows thixoextruded parts forged at a constant initial slug temperature of 1451 °C and at 40 mm/s, 100 mm/s and 215 mm/s. Let us consider a slab of material of 40 mm in diameter and small thickness along the extrusion direction. Based on Kim et al. (2001), and assuming velocity and strain rate to be uniform in the slab (as well as the incompressibility of the material), we calculated the average strain rates along extrusion direction, from the entrance to the exit of the die cone, for the ram speeds of interest. We found 50 s^{-1}, 125 s^{-1} and 313 s^{-1} for ram speeds of 40 mm/s,

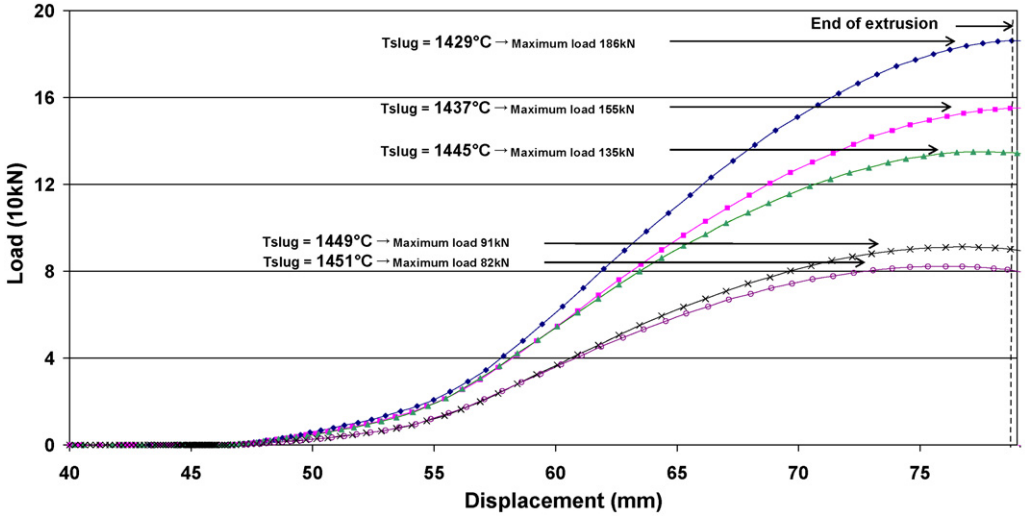

Fig. 6. Load–displacement signals during thixoextrusion for various initial slug temperatures (ram speed 215 mm/s and "cold" die).

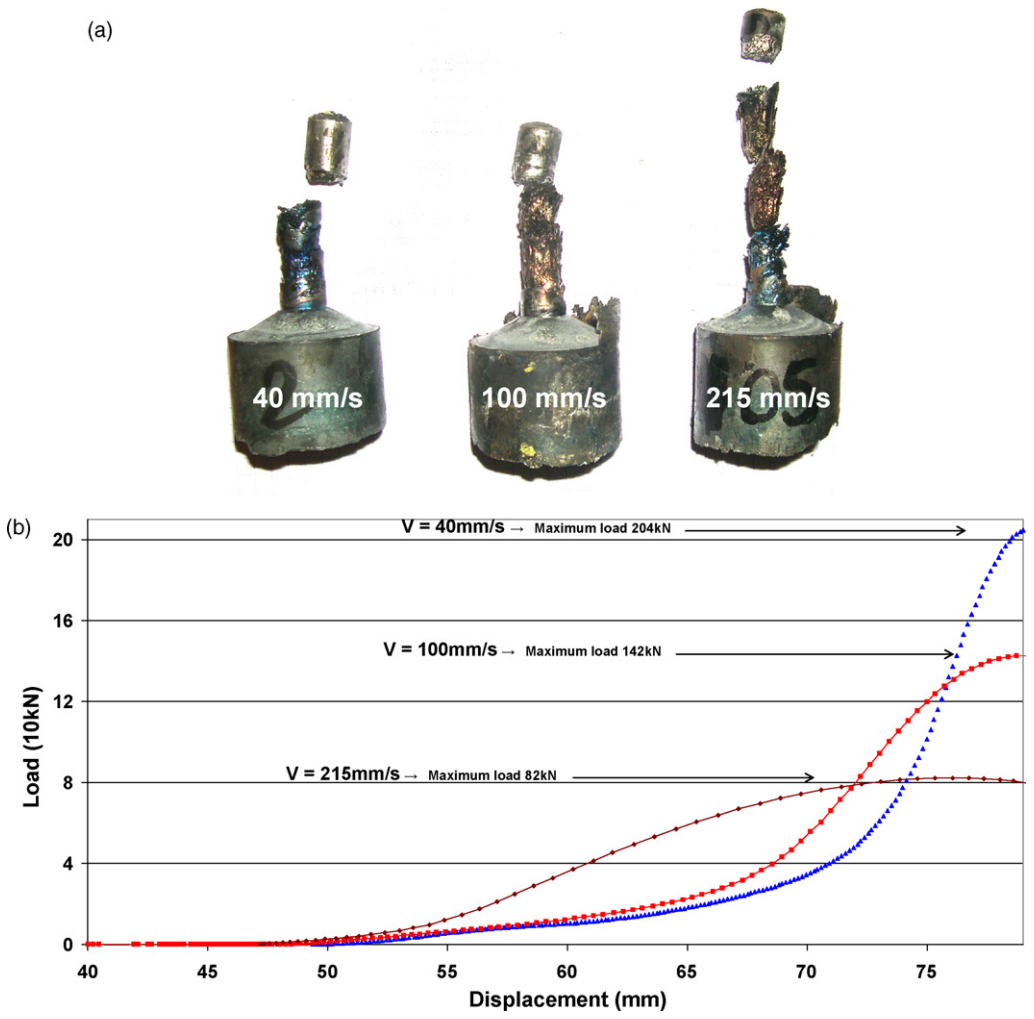

Fig. 7. Tests using various ram speeds and an initial slug temperature of 1451 °C ("cold" die): (a) thixoextruded parts and (b) load–displacement signals.

100 mm/s and 215 mm/s, respectively. Note that in these calculations, we ignored the strain of the material inside the container due to compression loading. Fig. 7b exhibits the load–displacement curves associated with tests using slugs at an initial temperature of 1451 °C. Fig. 7 shows load–displacement curves but for an initial slug temperature of 1429 °C.

When the initial slug temperature was equal to 1451 °C, a bad shape with wrenching was obtained whatever the ram speed

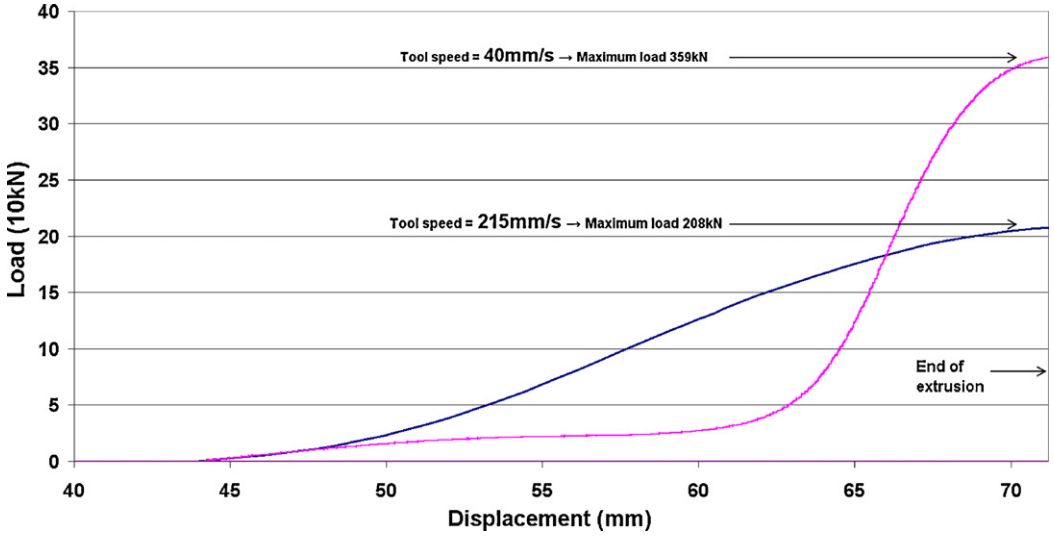

Fig. 8. Load–displacement signals during thixoextrusion for two ram speeds and an initial slug temperature of 1429 °C ("cold" die).

Fig. 9. Thixoextruded parts forged using a "cold" die and a "warm" die (ram speed 215 mm/s, initial slug temperature 1445 °C).

(Fig. 7a). When the initial slug temperature was equal to 1429 °C, we found that the extruded parts had an exact shape and a good surface state for the two desired ram speeds. These results are consistent with results described in Section 3.1. The initial slug temperature mainly controlled the quality of the component shape. For the two initial slug temperatures, we found that the load signal increased with the ram speed in the first part of the curves. This first part is associated with the filling of the container. Then, during the step of the die filling, the load signal was found much lower for the high ram speeds than for the low ram speeds. When the ram speed was 215 mm/s, the maximum load was around half the value of the load obtained when the ram speed was 40 mm/s for both temperatures. These results suggest that the behaviour of the material is different when the material is strained in the container and when it flows in the filling die (Fig. 8).

3.3. Impact of the die temperature

Fig. 9 shows the shape of extruded parts obtained for constant ram speed (215 mm/s) and initial slug temperature (1445 °C) and two die temperatures (20 °C and 400 °C).

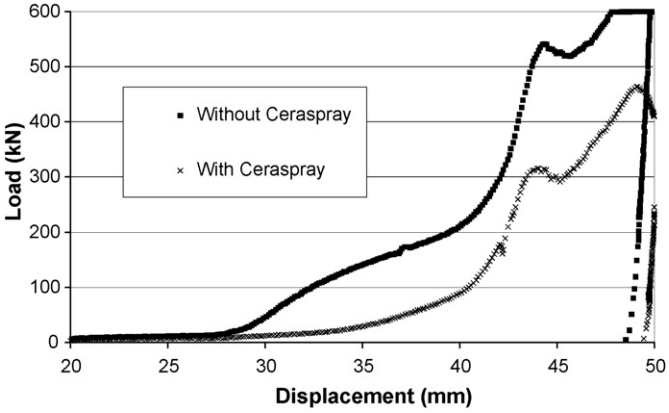

Fig. 11. Load–displacement signals during thixoextrusion for tests using or not using the Ceraspray©layer (ram speed 40 mm/s, initial slug temperature 1429 °C, press without damping located at Arts et Métiers ParisTech Metz).

Clearly, using the "warm" die improved the quality of the component shape. The extruded part displayed no wrenching and a good surface state. Concerning the load signals, we found that the maximum load slightly decreased when using the "warm" dies. The decrease was estimated to 25% (Fig. 9). The same trend was found with using the 215 mm/s ram speed. The decrease was estimated to 50%. These results are attributed to the reduction of heat losses when using the "warm" die (Fig. 10).

3.4. Impact of the Ceraspray©layer

Fig. 11 exhibits the impact of the Ceraspray© layer applied on the dies on the load–displacement curves. The Ceraspray©layer provided a significant decrease of the load (around 25%). This result may be attributed to (i) a reduction of heat losses since this ceramic may play the role of a thermal barrier at the tool–material interface, and/or (ii) a reduction of friction effects since the ceramic layer may play a lubricating role. These two effects would reduce the load by respectively decreasing the overall viscosity and the friction coefficient.

To go further on these interpretations, classical ring friction tests have been performed with a Ceraspray© layer C38 steels below the solidus at 900 °C and 1000 °C because it was very difficult to get reliable data with semi-solid materials. The results experimentally

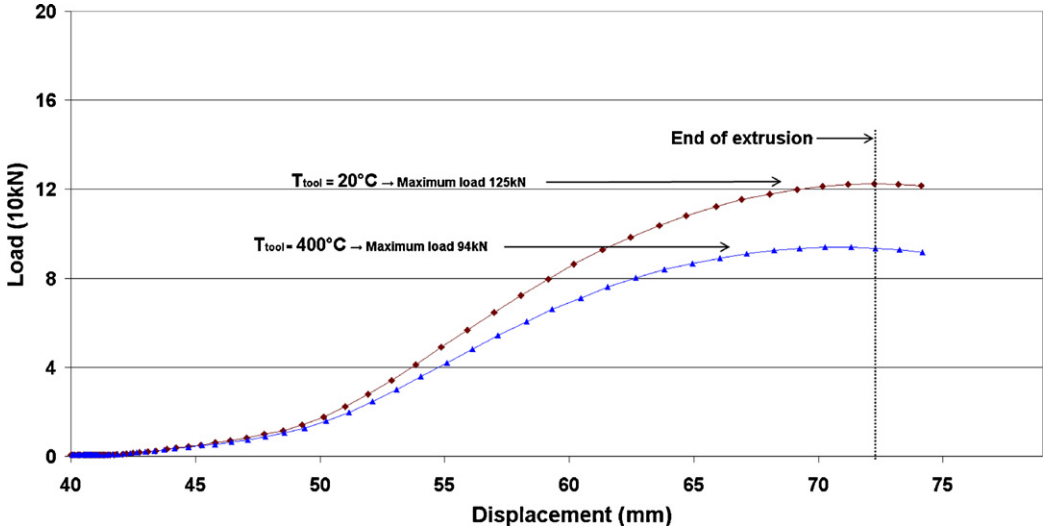

Fig. 10. Load–displacement signals during thixoextrusion for two die temperatures (ram speed 215 mm/s, initial slug temperature 1445 °C).

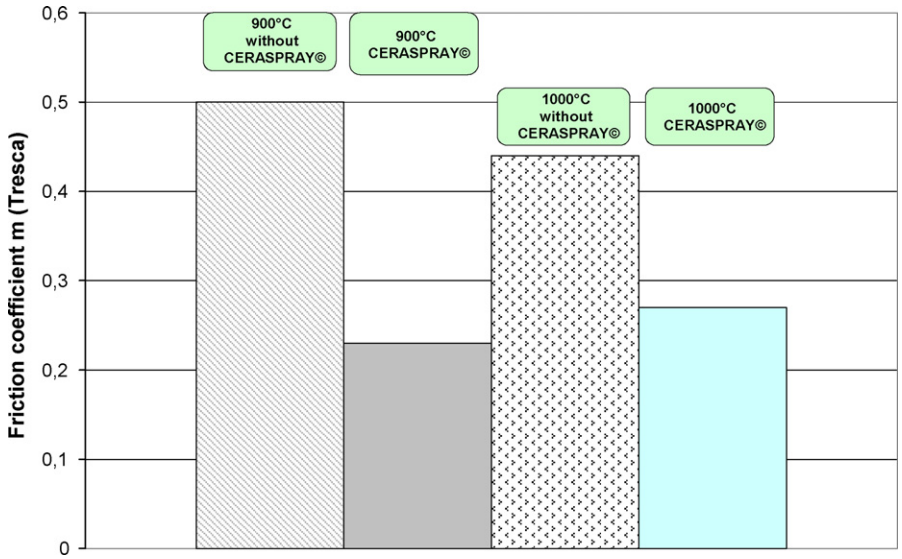

Fig. 12. Measured friction coefficient $\bar{m}$ (Tresca) from ring friction tests for two solid material temperatures and using or not using the Ceraspray©layer.

obtained are shown in Fig. 12. The Ceraspray© reduced efficiently the friction coefficient. For instance, the latter was found to be equal to 0.5 without the Ceraspray©layer and around 0.25 with the Ceraspray©layer at 900 °C. We expected the Ceraspray©layer to also reduce the friction effect at semi-solid temperature. However, it could not be the only reason for the decrease of load. Indeed, the friction coefficient has a major impact on the load–displacement signals when the material flows through the smallest diameter, i.e. when the contact surface becomes higher.

To go further in this work, we simulated extrusion tests using classical hot forging parameters for friction and constitutive behaviour. The constitutive equation was represented by Norton–Hoff law:

$$\underline{\underline{s}} = 2K(T,\bar{\varepsilon})(\sqrt{3}\dot{\bar{\varepsilon}})^{m-1}\underline{\underline{\dot{\varepsilon}}} \tag{1}$$

where $\underline{\underline{s}}$ and $\underline{\underline{\dot{\varepsilon}}}$ are the deviatoric stress and strain rate tensors, respectively. $\dot{\bar{\varepsilon}}$ is the Von Mises equivalent strain rate. m is the material strain rate sensitivity index. K is the material consistency which depends on temperature T and Von Mises equivalent strain $\bar{\varepsilon}$:

$$K(T,\bar{\varepsilon}) = K_0 * (\bar{\varepsilon} + \bar{\varepsilon}_0)^n * e^{\frac{\beta}{T}} \tag{2}$$

where K_0, $\bar{\varepsilon}_0$, n, β are materials parameters.

The friction law relates the shear stress τ and the normal stress σ_n as

$$\tau = \mu\sigma_n \quad \text{if} \quad \mu\sigma_n \leq \bar{m}\frac{\sigma_0}{\sqrt{3}} \tag{3}$$

and

$$\tau = \bar{m}\frac{\sigma_0}{\sqrt{3}} \quad \text{if} \quad \mu\sigma_n > \bar{m}\frac{\sigma_0}{\sqrt{3}} \tag{4}$$

where μ and $\bar{m}$ are the Coulomb and Tresca friction parameters, and σ_0 the initial yield stress of the material.

Table 3 gives numerical values for all parameters used in the numerical simulation.

Table 3
List of the parameters used for the simulations.

Consistency parameters				Friction parameters	
K_0 (MPa s)	n	β (1/K)	m	μ	$\bar{m}$
9	0.12	2450	0.17	0.4	0.25 or 0.5

Fig. 13 shows the load–displacement curves for simulated extrusion tests using the two extreme values (0.5 and 0.25) of friction parameters defined in Fig. 12. Clearly, the value of the friction coefficient only changes the predicted load–displacement signals during the last stage of the extrusion associated with the die filling. In contrast, the presence of the Ceraspray© layer changes the experimental load–displacement curve during all the forming process (Fig. 11). This comparison demonstrates that the ceramic layer plays both roles, namely that it acts as lubricant but also as thermal barrier.

4. Discussion

The experiments described above clearly showed that the initial slug temperature, the initial die temperature, the presence of the Ceraspray©layer, and the filling die velocity strongly impact the load required for filling as well as the shape of the extruded part.

4.1. Shape of extruded parts

Concerning the extruded parts, two typical kinds of shape were found: an exact shape with a very good surface state, and a non exact shape with a very bad surface state exhibiting wrenching, cracking and solidified liquid drops revealing a liquid/solid phase separation. The liquid/solid phase separation at the macro scale appears when increasing the initial slug temperature. The larger macro separation phenomenon (heterogeneous flow) was found at the highest initial slug temperatures. A critical temperature above which the flow is heterogeneous seems to exist. It was found around 1437 °C when using the "cold" die and the 40 mm/s ram speed. Kopp et al. (2004) and Li et al. (2005) presented the same kind of results obtained for other steel grades. Carrying out compression tests on aluminium alloys, Kang et al. (1999) also found similar results. The solid/liquid phase macro separation seems to require a high enough amount of liquid, or more precisely, a high enough amount of free liquid. Then, a preferred flow path develops dominated by the free liquid. Kang et al. (1999) also pointed out that the liquid/phase separation is smaller with increasing strain rate. Suery and Flemings (1982), Valette-Brives (1992) and Rouff (2003) suggested the existence of a critical strain rate above which homogeneous flow was observed. On the other hand, Li et al. (2005), who worked on stainless steel, mentioned that the critical temperature does not depend on strain and strain rate. The present investiga-

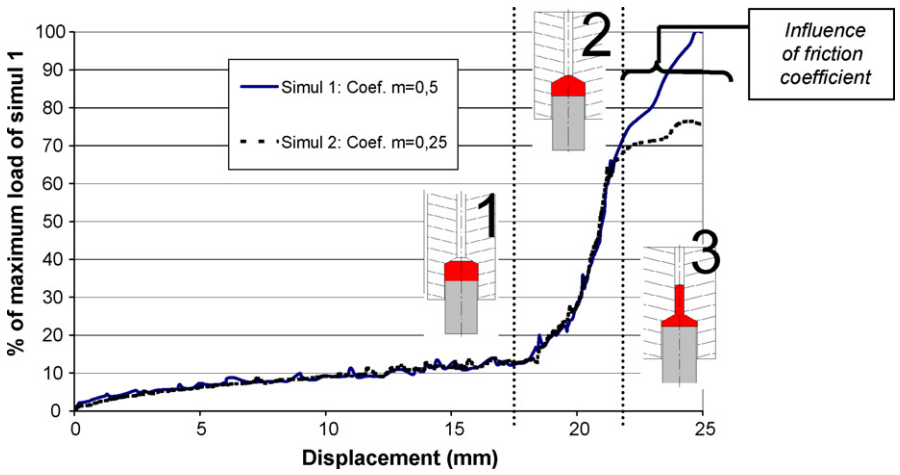

Fig. 13. Predicted load–displacement curves for extrusion associated with hot forging conditions for two Tresca coefficients (Forge2007®).

tion does not show any clear impact of ram speed on the nature (homogeneous or heterogeneous) of the flow. Using the initial slug temperature of 1451 °C probably requires reaching much higher ram speeds to observe a homogeneous flow. Other experiments with initial slug temperatures closer to the critical temperature of 1437 °C would be necessary to better analyse the ram speed effect on the nature of the flow. Finally, the liquid flow promotes the phase separation and so is dominated by the initial slug temperature. As shown by Favier et al. (2009, 2004) or Li et al. (2005), if temperature controls the overall amount of liquid, we expect the morphology of the semi-solid to also play a role since it controls the spatial distribution of both free and entrapped liquid.

Besides, using "warm" die and possibly the Ceraspray©layer gave extruded parts displaying an exact shape without wrenching. Both move the critical temperature towards higher values. For instance, Fig. 9 demonstrates that an exact shape of the extruded parts was obtained at an initial slug temperature of 1445 °C when using the "warm" die, while a bad shape was obtained when using the "cold" die. Fig. 15 exhibits simulated temperature fields within the specimen at the beginning of the extrusion step using "cold" and "warm" dies. The simulations were performed using the same parameters as in Section 3.4. The heat conduction transfer coefficient (between the die and the material) was considered equal to 20 kW/m^2 K. The initial distribution temperature before thixoforming is estimated by numerical simulation (Fig. 14). Fig. 15 reveals that a material layer where temperatures are lower than 1410 °C exists at the tool/material interface. According to Fig. 2, this "skin" is made of completely solidified materials. Its thickness is equal to 3.7 mm when the die is "cold" and to 2.6 mm when the die is "warm". In addition, temperatures in this layer are 100 °C higher when the die is "warm" than when the die is "cold". These results show that the heat losses at the tool/material interface create lower liquid fraction gradient in the cross-section when using the "warm" die. The amount of liquid and the material morphology is thus more uniform in the cross-section, resulting in a homogeneous material flow. A more thorough investigation of the flow is given in Becker (2008). Becker suggests that when the solid skin is formed in the container, the inside of the slug flows more rapidly than the surface of the slug. If the amount of liquid is high enough (at temperatures above the critical value), a liquid/solid phase separation occurs, namely the liquid flow activates. Some amount of liquid touches the die surface and solidifies in drops. This structure breaks under tensile stresses due to the relative flow combined with friction and/or to thermal contraction. These effects cause a disintegration of the microstructure as also found by Modigell and Pape (2008). Using "warm" die and possibly the Ceraspray©reduce the friction phenomena and the heat losses. As a result, it reduces significantly the phase separation phenomenon leading to extruded parts exhibiting an exact shape and a good surface state.

4.2. Load signal

Using the "warm" dies and/or the Ceraspray©layer enables to further reduce the load signal again because of the reduction of heat losses and friction phenomena. Besides, the load level was found to increase with decreasing the initial slug temperature. This result is expected and consistent with literature data for any semi-solids such as Sn–Pb alloys by Fan and Chen (2002), aluminium alloys by Kang et al. (1999) or Liu et al. (2003), or steels by Shimahara et al. (2006). It is attributed to the increase of the liquid fraction with increasing initial slug temperature. It can be pointed out in Fig. 2 that varying the slug temperature from 1429 °C to 1451 °C changes the liquid fraction from 0.04 to 0.2. Though we cannot directly apply these results to our thixoextrusion tests (see Section 2.1), these

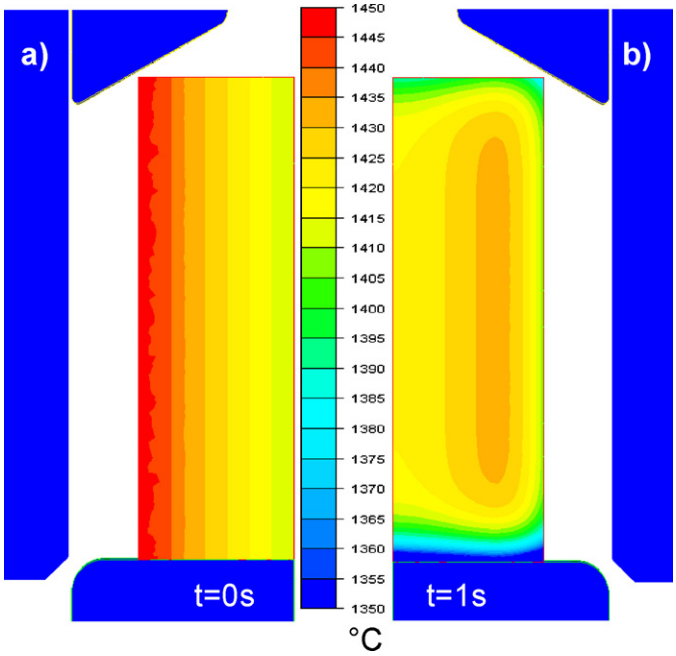

Fig. 14. temperature distribution in the slug heated by induction as simulated using Forge2008® (a) at the end of the heating and (b) after 1 s, corresponding to the transfer time of the slug.

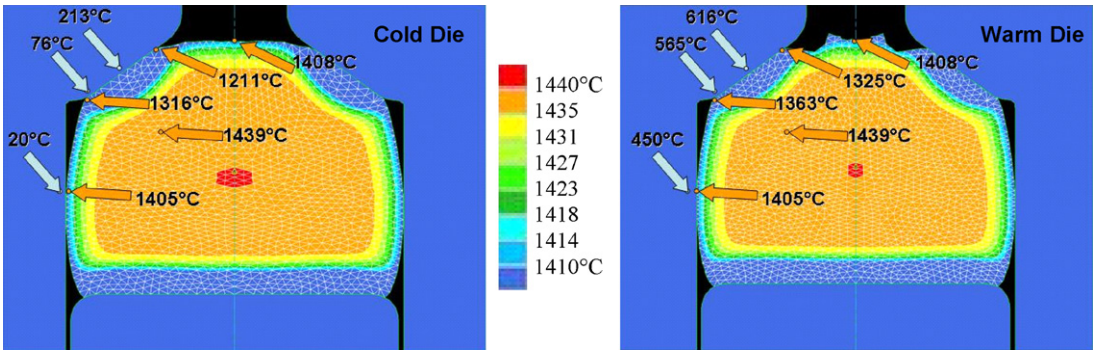

Fig. 15. Predicted temperature fields for the compression step of thixoextrusion tests using hot forging modeling obtained for the "cold" die and the "warm" die (ram speed 40 mm/s, initial slug temperature 1440 °C) (Forge2007®).

data indicate that the liquid fraction remains very low in the temperature range of interest. Fig. 5b displays the part obtained for an initial slug temperature of 1250 °C, namely for completely solid slug. The filling was not achieved for load values around 1000 kN (5–10 times higher than the load required to deform the semi-solid alloy). Clearly, the liquid, even in small quantities, eases the extrusion. Two reasons are suggested to explain the strong decrease of load with increasing initial slug temperature; see also Modigell et al. (2009). First, as shown by Atkinson (2005) and by Favier et al. (2009), though it is low the amount of liquid strongly affects the load level since the viscosity of the liquid is around 10^9 times lower than the viscosity of the solid. Second, when the solid/liquid phase separation at the macro scale occurs, the load signal is also expected to decrease because the liquid drives the flow and cracks appear at the specimen surface (Kang et al., 1999).

Besides, the load signal was found to increase for small displacements and then to decrease at higher displacements when the ram speed increases whatever the final shape of the part. For hot solids (below the solidus), the strain rate sensitivity parameter (power-law index when the behaviour is mathematically represented using a power-law relation) is around 0.2–0.3 (see e.g. Braccini et al., 2002). As a result, the stress increases along with the strain rate. So, below the solidus, the load signal for extrusion tests increases with the strain rate. Above the solidus (semi-solid state), Kang et al. (1999) and Liu et al. (2003), carrying out respectively compression tests and rapid compression tests on aluminium alloys, showed that the load signal decreased with the ram speed. Shimahara et al. (2006) performed compression tests on cold working X210CrW12 steel. Using the so-called "coat test" to avoid the early development of cracks and performing an inverse modelling, they found that the flow stress increased with the strain rate. Similarly, the highest stress was observed at the highest strain in stainless steel semi-solids (Li et al., 2005). So, all the experiments mentioned above, using a solid fraction higher than 0.5 as in our experiments, revealed positive strain rate sensitivity despite the loading path may be different. Using a Couette rheometer, Martin et al. (1995) analysed the shear rate sensitivity of the behaviour for high solid fraction (>0.6) semi-solid Sn–Pb under various structures. The behaviour at small strains (at the shear stress maxima) was found to have positive strain rate sensitivity whatever the structure. However, the steady state behaviour for stirred globular slurries exhibited negative shear rate sensitivity. McLelland et al. (1996) related also such negative shear rate sensitivity for stirred Sn–Pb slurries but for solid fraction lower than 0.5. This behaviour was attributed to a rapid

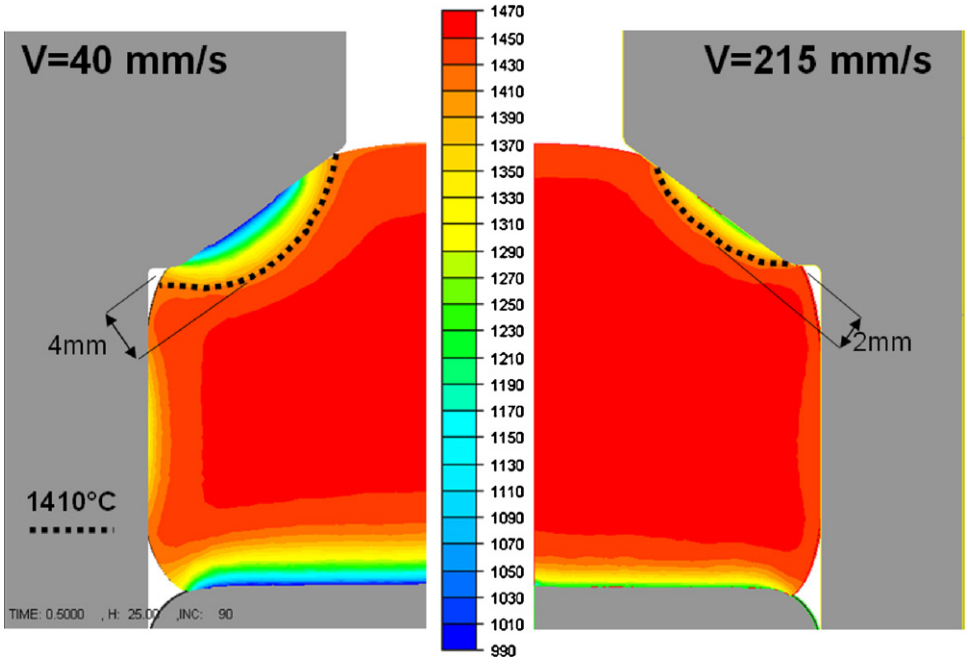

Fig. 16. Predicted temperature fields for the compression step of thixoextrusion tests using hot forging modeling obtained for two ram speeds ("cold" die, initial slug temperature 1410 °C).

breakdown of the internal structure (McLelland et al., 1996) and/or to the release of entrapped liquid (Martin et al., 1995). Apparently, we observe the same trends concerning the strain rate sensitivity. However, such desagglomeration process usually leads to a peak in load/stress (Favier et al. (2009)). No peak in load was observed in the present work (Figs. 7b, 8 and 16). Kang et al. (1999) found that the peak in compression stress disappears when the solid fraction is higher than 0.7 and when the strain rate increases for solid fraction equal to 0.7. The semi-solid response is thus similar to solid response obtained for hot compression experiments. In the literature experiments mentioned above (except Liu et al., 2003), the strain rates ranged from 0.1 s^{-1} to 50 s^{-1}. Consequently, it is much lower than the strain rates involved in our extrusion tests (higher than 50 s^{-1} see Section 3.2). As a result, following Kang et al. (1999) investigations, we should observe positive strain rate sensitivity. To better understand the negative strain rate sensitivity observed at high displacements, it is worth noticing that all literature experiments mentioned above (Li et al., 2005; Liu et al., 2003; Martin et al., 1995; McLelland et al., 1996) are considered as isothermal while our extrusion tests are non isothermal. Similarly to the simulated results obtained for "cold" and "warm" dies, we investigated the simulated temperature fields in relation to two ram speeds (40 mm/s and 250 mm/s). The simulations were obtained keeping all the other parameters constant (cold dies) (Fig. 16). The maximum thickness of the solidified skin was equal to 4 mm when using a ram speed of 40 mm/s and to 2 mm with a ram speed of 215 mm/s. The overall temperature in the skin was found higher and the temperature field more homogeneous for the high ram speed because the thixoforming time was found shorter. Accounting or these results, we suggest the following scheme to explain our experimental results.

Let us consider a homogeneous material flow. At the beginning of the forming, when the material is in the container, the load signal results from the viscoplastic behaviour of the solid skeleton. As a result, the semi-solid response displays positive strain rate sensitivity. Since the high solid fraction involved in our extrusion tests (>0.8), the solid skeleton is quite strongly bonded. Consequently, when the material fills the die, the load signal remains controlled by the solid skeleton. When the ram speed is high, the heat losses are small (Fig. 16) so that the thin solid skin is easily broken during forming. We may expect the deformation at such high strain rate to lead to the break down of a part of the solid bonds inside the skeleton. In addition, viscous dissipation may produce a slight heating of the material. As a result, the cohesion of the solid skeleton is slightly weakened compared to its initial state. Consequently, the filling of the die requires a quite low load. When the ram speed is lower, the heat losses enhance the thickness of the solid skin and the temperature gradient in the cross-section of the slug. As a result, the skin and the overall skeleton are more resistant explaining the increase of the load signal associated to the die filling.

Let us consider now a heterogeneous material flow. When the material is in the container, the phase separation has not occurred yet. So, the same scheme explains the first part of the load–displacement curves and the associated positive strain rate sensitivity. When the material fills the die, its response is now dominated by the liquid flow. When the ram speed is low, here again, liquid may solidify because of heat losses so that the load signal is high. When the ram speed is higher, a bigger amount of liquid participates in the flow since the overall amount of liquid but also the amount of free liquid (disagglomeration process of the solid skeleton) are larger. As a result, the load required to fill the die is lower. The proposed scheme explains the change in strain rate sensitivity during the forming and the differences with literature results.

All the features mentioned above are significant for industrial thixoforming. One of the interests of thixoforming with regard to hot forging is to reduce the forming force. To get a lower forming force, the results discussed above reveal that one may increase the initial slug temperature. However, the flow risks being heterogeneous, inducing a bad shape of the part. One may also increase the ram speed. Fig. 17 shows two extruded parts obtained for the same load signal. The first part was obtained using an initial slug temperature of 1451 °C and a ram speed of 40 mm/s, and it displays wrenching at the surface. The second part was obtained with an initial slug temperature of 1429 °C which is lower than the critical temperature and a ram speed of 215 mm/s. In this case, the part has the exact shape with a smooth surface. These results demonstrate that the ram speed, the initial temperature of the slug and the die can be adjusted to get a part exhibiting an exact shape with a low forming force.

Fig. 17. Two thixoextruded parts having a bad shape (left) and an exact shape (right) forged at the same load (200 kN) but for different initial slug temperature and ram speed ("cold" die).

5. Conclusions

Extrusion tests were conducted on semi-solid C38 steels. This paper concentrates on high solid fractions. Four different process parameters were here studied: the initial slug temperature, the die temperature, the ram speed and the presence of a Ceraspray©layer at the tool/material interface. The extruded parts have an exact shape and a good surface state only if the temperature is inferior to a critical value. This critical temperature is not an intrinsic material property since its value depends on die temperature and the presence of the Ceraspray©layer. Two kinds of flow are highlighted: a homogeneous flow controlled by the behaviour of the solid skeleton characterized by a positive strain rate sensitivity and a non homogeneous flow (macro liquid/solid phase separation) dominated by the flow of the free liquid. Heat losses affect the cohesion and the resistance of the solid skeleton and consequently the load signal. We found that with decreasing the ram speed, heat losses increase so that the overall consistency of the material improves, leading to apparent negative strain rate sensitivity. We demonstrated that a low forming force involved during thixoforming as compared to that in conventional hot forgings can be obtained in order to produce a component showing a good shape and surface state by using a "warm" die coated in a Ceraspray©layer and a suitably high ram speed.

Acknowledgements

The authors would like to sincerely thank the University of Liege, especially Dr Ahmed Rassili, for giving them the opportunity to use

their hydraulic press to perform these experiments, and for their support of this work.

References

Atkinson, H.V., 2005. Modelling the semisolid processing of metallic alloys. Progress in Materials Science 50 (3), 341–412.

Balitchev, E., Meuser, H., Neuschutz, D., Bleck, W., 2004. Experimental investigations and computer simulation of the liquid fraction evolution during the solidification of alloys suitable for semi-solid processing. Steel Research International 75 (1), 13–19.

Becker, E., 2008, Investigations expérimentales et numériques pour l'identification des paramétres clefs du thixoforgeage de l'acier sur le produit mis en forme, Thesis, ENSAM, Metz.

Becker, E., Bigot, R., Langlois, L., 2009. Thermal exchange effects on steel thixoforming processes. International Journal of Advanced Manufacturing Technology, 1–12.

Bigot, R., Favier, V., Rouff, C., 2005. Characterization of semi-solid material mechanical behavior by indentation test. Journal of Materials Processing Technology 160, 43–53.

Braccini, M., Martin, C.L., Tourabi, A., Brechet, Y., Suery, M., 2002. Low shear rate behavior at high solid fractions of partially solidified Al–8 wt.% Cu alloys. Materials Science and Engineering A—Structural Materials Properties Microstructure and Processing 337 (1–2), 1–11.

Cezard, P., Sourmail, T., 2008. Thixoforming of steel: a state of the art from an industrial point of view. Semi-Solid Processing of Alloys and Composites X 141–143, 25–35.

Fan, Z., Chen, J.Y., 2002. Modelling of rheological behaviour of semisolid metal slurries. Part 2. Steady state behaviour. Materials Science and Technology 18 (3), 243–249.

Favier, V., Rouff, C., Bigot, R., Berveiller, M., 2004. Micro-macro modelling of the isothermal steady-state behaviour of semi-solids. International Journal of Forming Processes 7, 177–194.

Favier, V., Bigot, R., Cezard, P., 2009. Transient and non-isothermal semi-solid behaviour: a 3-D micromechanical modeling. Material Science and Engineering A 1–2, 8–16.

Flemings, M.C., 1991a. Behaviour of metal alloys in the semisolid state. Metallurgical and Materials Transactions A 22 (5), 957–981.

Flemings, M.C., 1991b. Behaviour of metal alloys in the semisolid state. Metallurgical and Materials Transactions B 22 (3), 269–293.

Gibbs, J.W., Mendez, P.F., 2008. Solid fraction measurement using equation-based cooling curve analysis. Scripta Materialia 58 (8), 699–702.

Hirt, G., Shimahara, H., Seidl, I., Kuthe, F., Abel, D., Schonbohm, A., 2005. Semi-solid forging of 100Cr6 and X210CrW12 steel. Cirp Annals-Manufacturing Technology 54 (1), 257–260.

Hirt, G., Khizhnakova, L., Baadjou, R., Knauf, F., Kopp, R., 2009. Semi-solid forging aluminium and steel, Introduction and overview. In: Hirt, G., Kopp, R. (Eds.), Thixoforming: Semi-solid Metal Processing. Wiley, pp. 1–27.

Jung, H.K., 2000. The induction heating process of semi-solid aluminium alloys for thixoforming and their microstructure evaluation. Journal of Materials Processing Technology 105 (1–2), 176–190.

Jung, H.K., Kang, C.G., Moon, Y.H., 2000. Induction heating of semisolid billet and control of globular microstructure to prevent coarsening phenomena. Journal of Materials Engineering and Performance 9 (1), 12–23.

Kang, C.G., Choi, J.S., Kim, K.H., 1999. The effect of strain rate on macroscopic behavior in the compression forming of semi-solid aluminium alloy. Journal of Materials Processing Technology 88, 159–168.

Kang, C.G., Seo, P.K., Jung, H.K., 2003. Numerical analysis by new proposed coil design method in induction heating process for semi-solid forming and its experimental verification with globalization evaluation. Materials Science and Engineering A—Structural Materials Properties Microstructure and Processing 341 (1–2), 121–138.

Kapranos, P., Kirkwood, D.H., Sellars, C.M., 1993. Semisolid Processing of Aluminum and High Melting-Point Alloys. Proceedings of the Institution of Mechanical Engineers Part B—Journal of Engineering Manufacture 207 (1), 1–8.

Kim, N.H., Kang, C.G., Kim, B.M., 2001. Die design optimization for axisymmetric hot extrusion of metal matrix composites. International Journal of Mechanical Sciences 43 (6), 1507–1520.

Koke, J., Modigell, M., 2003. Flow behaviour of semi-solid metal alloys. Journal of Non-Newtonian Fluid Mechanics 112 (2–3), 141–160.

Kopp, R., Shimahara, H., Schneider, J.M., Kurapov, D., Telle, R., Munstermann, S., Lugscheider, E., Bobzin, K., Maes, M., 2004. Characterization of steel thixoforming tool materials by high temperature compression tests. Steel Research International 75 (8–9), 569–576.

Li, J.-Y., Sugiyama, S., Yanagimoto, J., 2005. Microstructural evolution and flow stress of semi-solid type 304 stainless steel. Journal of Materials Processing Technology 161 (3), 396–406.

Liu, T.Y., Atkinson, H.V., Kapranos, P., Kirkwood, D.H., Hogg, S.C., 2003. Rapid compression of aluminum alloys and its relationship to thixoformability. Metallurgical and Materials Transactions A—Physical Metallurgy and Materials Science 34A (7), 1545–1554.

Martin, C.L., Brown, S.B., Favier, D., Suery, M., 1995. Shear deformation of high solid fraction (>0.60) semi solid Sn–Pb under various structures. Materials Science and Engineering A202, 112–122.

McLelland, A.R.A., Anderson, P.R.G., Atkinson, H.V., Kirkwood, D.H., 1996. The application of ceramic moulds to semi-solid metal forming. In: Proceeding of the 4th International Conference on Semi-Solid Processing of Alloys and Composites, Sheffield, pp. 274–277.

Modigell, M., Pape, L., 2008. A Comparison of measuring devices used to prevent wall slip in viscosity measurements of metallic suspensions. Semi-Solid Processing of Alloys and Composites X 141–143, 307–312.

Modigell, M., Pape, L., Vasilic, K., Hufschmidt, M., Hirt, G., Shimahara, H., Baadjou, R., Buhrig-Polaczek, A., Afrath, C., Kopp, R., Ahmadein, M., Bunck, M., 2009. Modelling the flow behaviour of semi-solid metal alloys. In: Hirt, G., Kopp, R. (Eds.), Thixoforming: Semi-solid Metal Processing. Wiley, pp. 169–217.

Omar, M.Z., Atkinson, H.V., Palmiere, E.J., Howe, A.A., Kapranos, P., 2004. Microstructural development of HP9/4/30 steel during partial remelting. Steel Research International 75 (8–9), 552–560.

Omar, M.Z., Palmiere, E.J., Howe, A.A., Atkinson, H.V., Kapranos, P., 2005. Thixoforming of a high performance HP9/4/30 steel. Materials Science and Engineering A—Structural Materials Properties Microstructure and Processing 395 (1–2), 53–61.

Puttgen, W., Bleck, W., Hirt, G., Shimahara, H., 2007. Thixoforming of steels—a status report. Advanced Engineering Materials 9 (4), 231–245.

Quaak, C.J., 1996. Rheology of partially solified aluminium alloys and composites. Thesis, Technische Universiteit, Delf, Holland.

Rassili, A., Robelet, M., Fischer, D., 2006. Thixoforming of carbon steels: inductive heating and process control. Semi-Solid Processing of Alloys and Composites 116–117, 717–720.

Rouff, C., Bigot, R., Favier, V., Robelet, M., 2002. Characterization of thixoforging steel during extrusion tests. In: Proceedings of the 7th Semi-solid Processing of Alloys and Composites, Tsukuba, Japon, September 24–28, vol. A-56, pp. 355–360.

Rouff, C., 2003. Contribution à la caractérisation et à la modélisation du comportement d'un acier à l'état semi-solide. Application au thixoforgeage, Thesis, ENSAM, Metz.

Shimahara, H., Baadjou, R., Kopp, R., Hirt, G., 2006. Investigation of flow behaviour and microstructure on X210CrW12 steel in semi-solid state. Semi-Solid Processing of Alloys and Composites 116–117, 189–192.

Suery, M., Flemings, M.C., 1982. Effect of strain rate on deformation behaviour of semi solid dentritic alloys. Metallurgical Transactions 13A, 1809–1819.

Valette-Brives, E., 1992. Mise en forme d'aciers à l'état semi-solide: étude expérimentale et modélisation, Thesis, Ecole Nationale Supérieure de Mines de Paris/Ecole Nationale Supérieure de Mines de Saint-Etienne, France.